Collider-Accelerator Department

BROOKHAVEN NATIONAL LABORATORY

Building 911B – P.O. Box 5000
Upton, NY 11973-5000
Phone 631 344 7124
Fax 631 344 5568
beavis@bnl.gov
www.bnl.gov

managed by Brookhaven Science Associates
for the U.S. Department of Energy

Memo

Date: *May 11, 2015*

To: *C. Schaefer (IRR team Leader), RSC, D. Kayran, and I. Ben-Zvi*

From: *D. Beavis* *& C. Cullen*

Subject: *ERL Beam Fault Studies and Maximum Beam Power*

Introduction

The IRR wrote pre-start item 2.3.1 "Determine a maximum fault study beam power and ensure this is clearly documented in the commissioning Sequence and Fault Study Plans." The purpose of this report is to address this finding by the IRR. The IRR did not state what their concern was but it is assumed that it is machine damage and not safety.

Three identified issues with localized beam loss are listed below:

1. Damaging the item being struck with the electron beam. The items planned are either end flanges to straight sections in the vertical chicane, scrapping the beam pipe in a vacuum box, and striking a piece of intrusive instrumentation such as copper mirror.
2. Damaging the beam pipe or end flanges could potentially lead to damage of the machine through loss of vacuum. Damage of a mirror or the YAG crystal could result in the need to open the vacuum and replacing the mirror or crystal.
3. High temperatures induced on surfaces may cause increased vacuum pressure and result in valve closure and potentially cathode damage if not properly protected from the pressure rise.

There is no simple single solution for the maximum beam power. There are several different issues that impact what the desirable maximum should be including the various objects being struck, the material composition, the potential outgassing of the material, and the time required to conduct radiation measurements. An option is to increase the beam power allowed to strike an object but for a shorter time period then required to achieve a steady state temperature.

In consultation with the vacuum personnel it is unlikely that a definite answer can be provided for the loss of vacuum due to out gassing. The beam pipe system has not been baked and they would be concerned with any temperatures over 200° C. Temperature changes at conflat knife edges are a potential concern. Addressing the vacuum issues will be an empirical incremental process.

It is proposed that pre-start finding 2.3.1 should be replaced with the following:

2.3.1 Incorporate in the Commissioning Sequence and Fault Study Plans the consideration of potential machine damage during the fault studies. Review should be conducted at each stage of the commissioning to ensure that the machine is protected.

A post start item should be added that recommends review of any thermal and vacuum issues caused by the fault studies. A post start item is proposed:

2.4.1 Review any thermal measurements and vacuum issues caused by the beam fault studies.

The goal of beam fault studies is to verify the shielding design to a sufficient degree to ensure the C-AD shielding policy is satisfied by the design. This requires being able to ensure that radiation monitors have the correct sensitivity to various beam faults and the areas external to the shielding are properly protected. This usually requires the detection of dose external to the shielding, but it is possible to add detectors internal to the enclosure and then extrapolate the measurements using acceptable techniques.

A secondary use of faulting the beam is the testing of instrumentation and the establishment of Machine Protection System (MPS) set-points.

The reminder of this report will focus on the thermal analysis of beam striking various machine components.

Thermal Analysis for Beam Faults

The thermal analysis is conducted in two stages. First the energy deposition caused by the beam is calculated using MCNPX[1]. Data files providing the MeV/cm^3 are provided for a set of volumes in the geometry. This input is then used in ANSYS 16.0 for thermal analysis[2] to calculate either the steady state or the transient state of the system. Typically approximations are used to make the analysis efficient and reduce manpower for the initial setup.

The calculations for the 3.5 MeV electron beam use a beam distribution that is Gaussian in x and y. The x and y sigma have been made equal and have been set to 3 mm[3]. For 25 MeV it is assumed that either the beam can be enlarged to 3mm or 1mm beam sizes are used. The particles are assumed to be parallel to the beam direction. The energy deposition in an object is then tallied using an appropriate mesh in MCNPX. The output data is slightly processed and an ASCII file is provided for the thermal analysis. The thermal analysis accounts for vacuum on the inside of the beam pipe. Processes to distribute deposited energy include radiation, conduction, and convection. Several cases were studied to represent expected conditions during beam fault studies.

---

[1] MCNPX 2.7c, D. PELOWITZ (ed.), “MCNPX User’s Manual”, Version 2.7.0, Los Alamos National Laboratory, LA-CP-11-00438 (2011).
[2] ANYSY reference *****
[3] The beam size used is based on discussions with D. Kayran.

A. Stainless Steel Flange

The first Faraday cup is a stainless steel flange. This flange is at the end of the straight segment from the gun. The first three segments of the vertical chicane have flanges at the end which can be struck with beam if the preceding dipole is off. The flanges will be used for beam fault studies. The three flanges may have thermocouples added[4], although they may not be ready for the first beam tests. The thermocouples for the second and third flange are expected to be moved to the upstream crouch area of the dipole vacuum box. This area is a possible location for beam scrapping during normal operations. The thermocouples will be readout by the Machine Protection System (MPS). The readout can be used to interactively monitor the temperature and to provide a machine protection interlock.

The beam is assumed to strike the flange in the center. The flange is 17.4 mm thick and has a radius of 70 mm. The problem has azimuthal symmetry, which allows for faster computation and easier setup. The energy deposition is computed in radial rings with 1 mm thickness for 40 mm. The energy deposition is displayed in Figure I. Essentially all the energy is deposited in a few 10s of mm in radius and was the reason for truncating the energy deposition calculation at a radius of 5 cm. The Gaussian structure of the beam is evident at small radii and after 1.2 cm the power density is dominated by photons and scattered electrons. The energy deposition[5] is integrated over the entire thickness of the flange. The thermal analysis assumed that the energy was evenly deposited in the inner 3 mm of the flange thickness. The steady state solution for 100 Watts of beam on the flange is shown in Figure II.

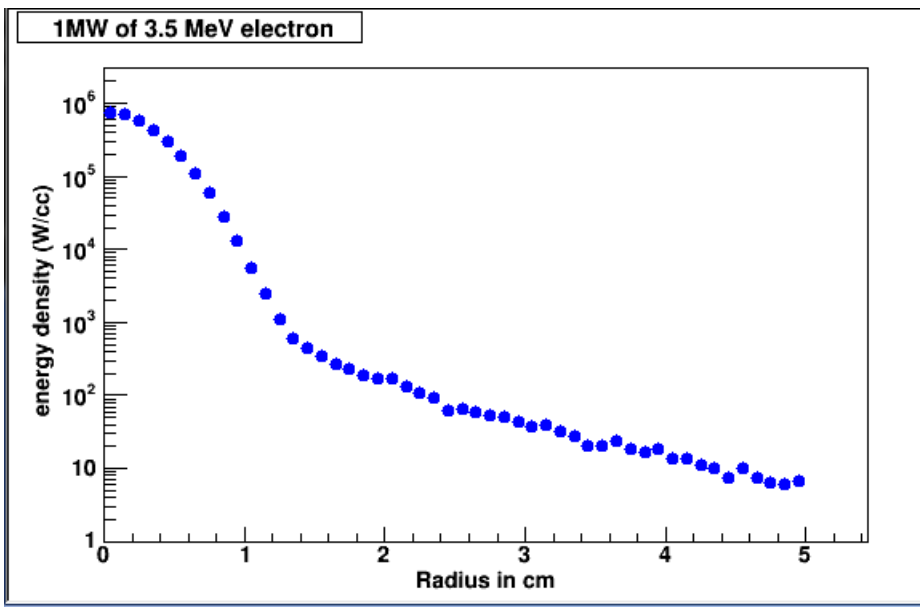

Figure I: The power deposition in Watts per cc assuming 1 MW of 3.5 MeV electrons incident on a stainless steel flange. The power density is integrated over the 1.74 cm thickness of the flange and the beam size has a sigma of 3mm.

[4] Some flanges may have additional instrumentation added and the thermocouples may not be present.
[5] For 3.5 MeV 94% of the beam energy is deposited into the flange.

SS Flange Beamstop, 3.5 MeV, Steady-State

100 Watt Case

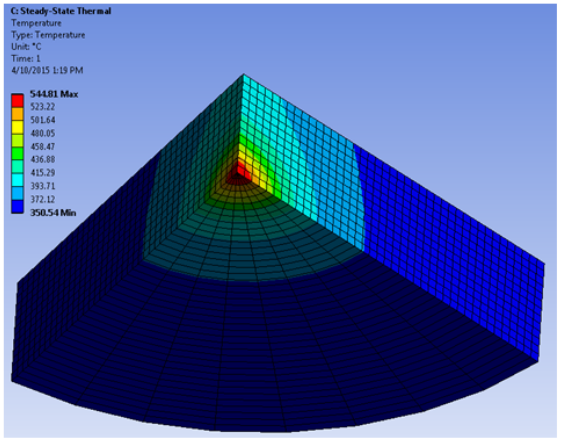

Results Summary

Nominal Case, W	Watts In	Temp Range, °C
1	.94	32-34
10	9.4	100-124
100	93.3	350-545

Figure II: Steady state solutions for 3.5 MeV electrons with a 3mm sigma in x and y striking a stainless steel flange.

The steady state solution for 100 Watts has a large temperature differential between the center of the flange (545° C) and the outside radius of the flange (350° C). This condition will likely be unsuitable for vacuum and the integrity of the knife edge. A transient solution was run for 10 minutes to determine if short bursts with 100 Watts of beam power would be suitable. The results are shown in Figure III.

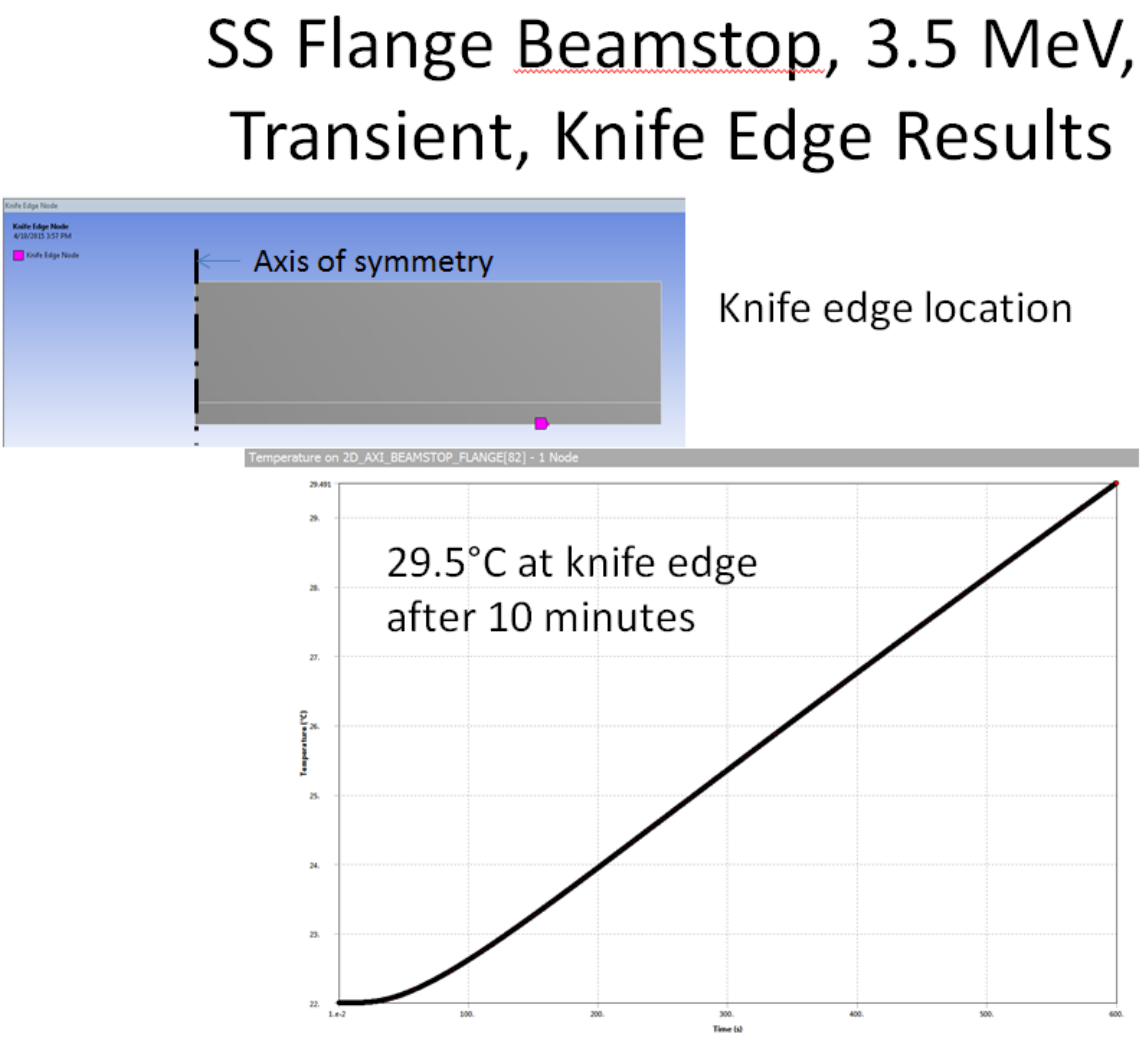

Figure III: Temperature at the knife edge of the conflate flange as a function of time for a 3.5 MeV beam with 100 W of power.

The knife edge will reach a steady sate temperature of 350^0 C but for short periods of time such as ten minutes the knife edge will only reach 29° C and the center of the flange 54° C. With appropriate precaution it should be possible to expose the flange at 100 Watts of continuous beam for time periods of 10 to 20 minutes. Even longer periods may be possible but the action should proceed carefully.

The fault studies will not use the integrated beam on target effectively if the beam continuously strikes the target. There are typically two time periods used for fixed locations for the radiation measurements, 30 seconds or 120 seconds. The longer time enables reducing the minimum detectable level and uncertainty if necessary. It would be appropriate to leave the beam off until the RCTs are prepared to make a measurement and then turn the beam on for a time period slightly longer than required for the measurement. After the radiation measurement the beam should be turned off until the RCTs are repositioned at the next location. This will reduce the heating and vacuum issues for the beam fault studies.

Simulations on the flanges were not conducted for 25 MeV as there are none in the system that could easily be used. There may be a few small flanges at the downstream end of the port pipe in the dipole Al vacuum boxes.

B. Profile Monitors and Copper Mirrors

The Profile Monitors employ a YAG crystal that is perpendicular to the beam to generate an image of the beam profile. A copper mirror downstream of the crystal is tilted at 45° and reflects the light perpendicular to the beam through an optical window to be viewed by a digital camera. The PM system can be moved into or out of the beam. The MPS demands that the PM is either completely inserted or completely removed for the beam permit. The YAG crystal and the mirror are supported by a substantial metal box which is not intended to be in the beam at any time. The copper mirror provides an opportunity to produce a well-defined beam loss.

There are five PMs that may be useful for beam fault studies. Figure IV displays the locations of instrumentation in the ERL. The PM before the Faraday cup (flange) may be more useful for the

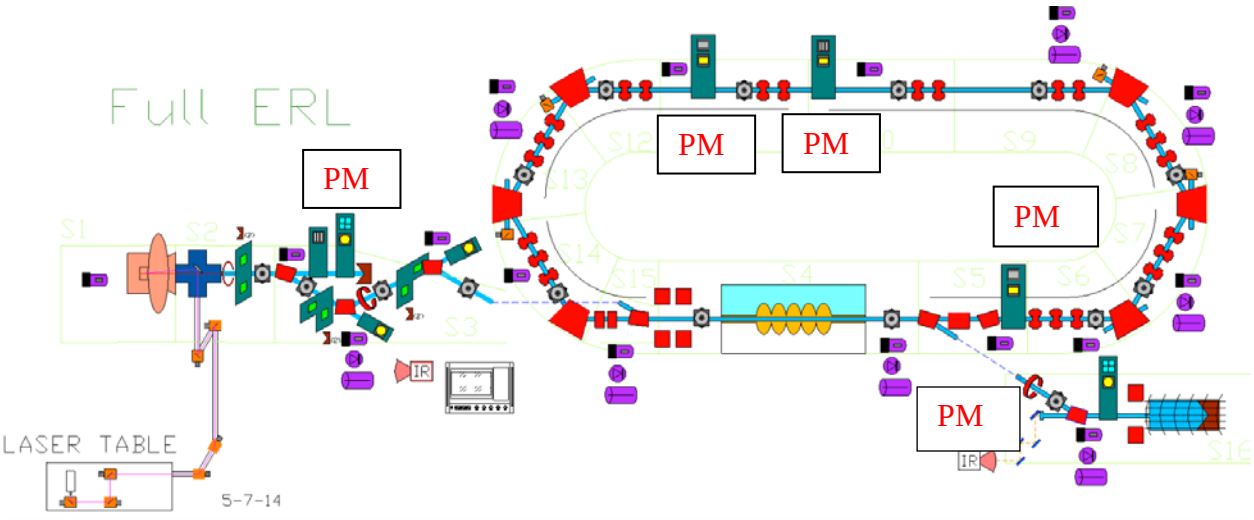

Figure IV: Locations of the instrumentation in ERL. The five PMs that could be useful for beam fault studies are labeled.

beam fault studies. The copper mirror may represent less risk to the vacuum compared to the flange via less outgassing and reduction in potential damage to the knife edge seal. However, this will need to be examined verses the risk to the YAG crystal. Vacuum issues can be examined during initial low power studies. The PM downstream of the extraction channel could be used fault studies at both injection energy and accelerated beam energy from the five-cell cavity. One of the PMs on the back side of the loop[6] could be useful for a fault study in the back segment of the loop. Finally, a PM in front of the beam dump could be used for fault studies in the extraction channel. The box has been located in the segment that is after the first extraction dipole.

[6] The preference would most likely be the first one rather than the second.

The copper mirrors have a thickness of 0.95 cm and a radius of 3.1 cm. The mirror is attached to the frame that holds both the YAG crystal and provides coupling to the insertion mechanism. Figure V displays a view of a mirror/crystal assembly. The YAG crystal nor the copper mirror are expected to have good thermal contact with the frame. The thermal conductivity is ignored in the analysis and only radiation to other surfaces within the vacuum is considered in the thermal analysis.

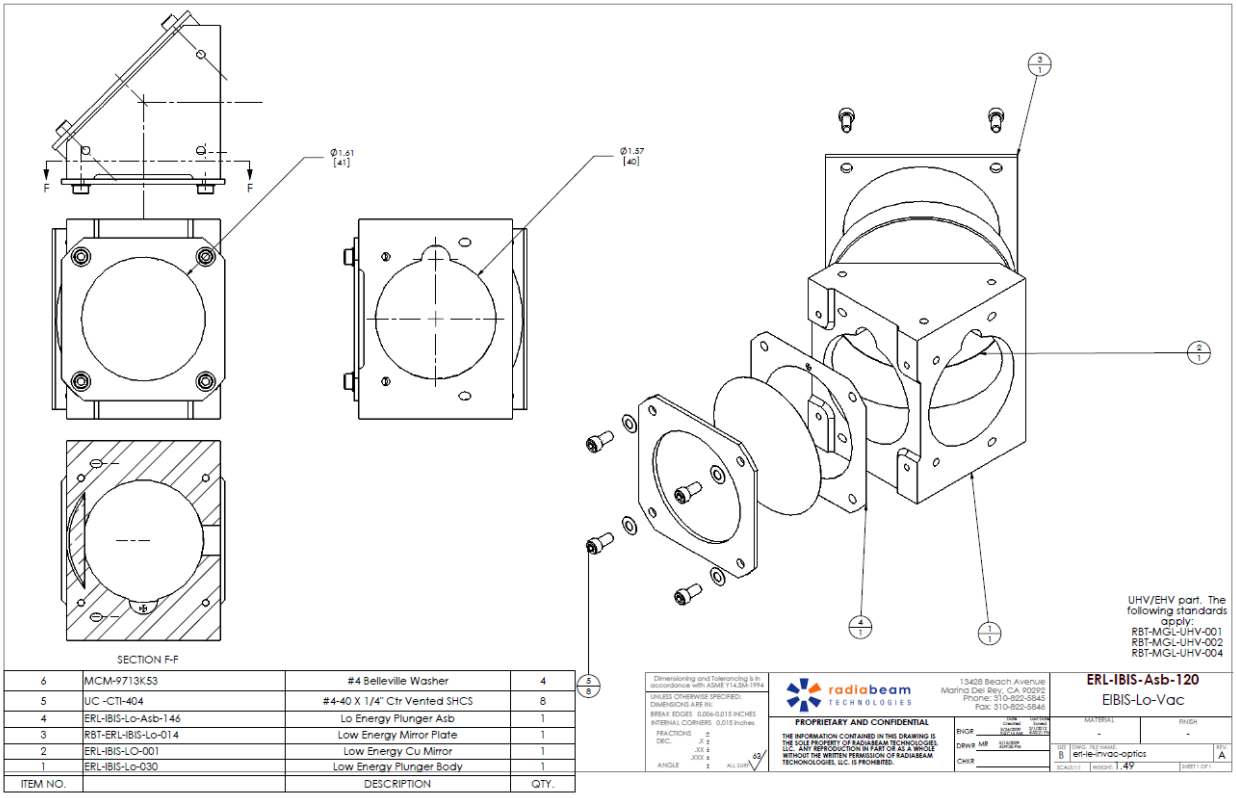

Figure V: YAG crystal and mirror frame assembly.

The steady state results for the copper mirror are displayed Figure V. The good thermal properties of the copper allow the small area power deposition to be spread throughout the mirror volume. There are only small differences in temperature from the center of the mirror and the outside radius. Although the mirror gets hot for 100 Watts of beam[7] the temperature rise is 50° C in ten minutes. It would be practicable to operate with continuous beam of 100 Watts for periods exceeding twenty minutes with the mirror reaching only 100° C and 35 minutes to reach 200° C.

[7] 91% (91 Watts) of the beam energy is deposited in the copper disc. If the disc was rotated 45 degrees this would increase to close to 100%.

Copper Mirror, 3.5 MeV, Steady-State

10 Watt Case

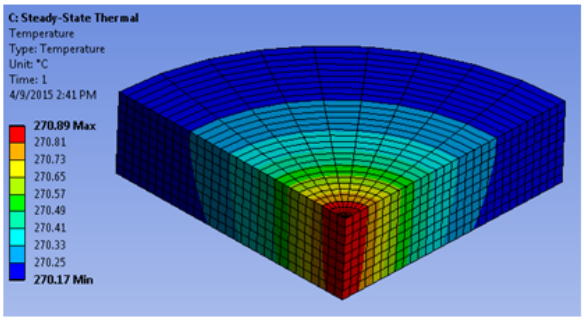

Results Summary

Nominal Case, W	Watts In	Max Temp, °C
1	.88	80
10	8.72	271
100	86.9	680

Figure VI: Steady state solution for the copper mirror.

The YAG crystal[8] is 100 microns thick. Assuming the entire mass is yttrium then the 3.5 MeV energy lost in the YAG is less than 0.16 MeV per electron with an energy density of 0.36 MeV/gm per electron in the central portion of the beam peak. This should be compared with the copper which will have 0.42 MeV/gm per electron in the central portion of the beam peak. However, the thermal properties of copper are much better than YAG. It was decided that a thermal analysis of the YAG crystal would be conducted. The power density deposited as a function of radius for the 3.5 MeV beam is shown in Figure VII. 1.7% of the initial beam power is deposited in the YAG. The tail above a radius of 1.5 cm may be caused by scatter from the surrounding stainless steel beam pipe. The steady state temperature profile is shown in Figure VIII. The center of the crystal reaches 58° C compared to 271° C for the copper disk. It does appear that the YAG crystal coupled with the copper mirror could be used[9] in beam fault studies.

[8] The chemical composition is $Y_3Al_5O_{12}$ with a density of 4.55 g/cc, thermal conductivity of 11.2 W/(m-k), a specific heat capacity of 0.59 J/(g-K), emissivity of 0.7, and a melting point of 1965° C.
[9] There may be mechanical issues that will need to be addressed for the YAG.

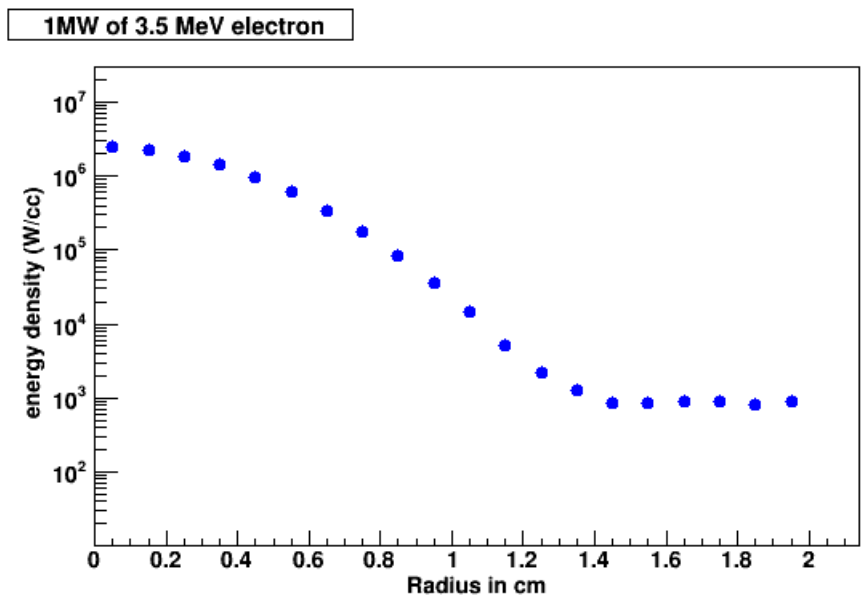

Figure VII: Power density as a function of radius for a 3.5 MeV electron beam striking a YAG crystal. The beam has a sigma of 0.3cm and a beam power of 1 MW. The crystal is 2 cm in diameter and has a thickness of 0.01 cm

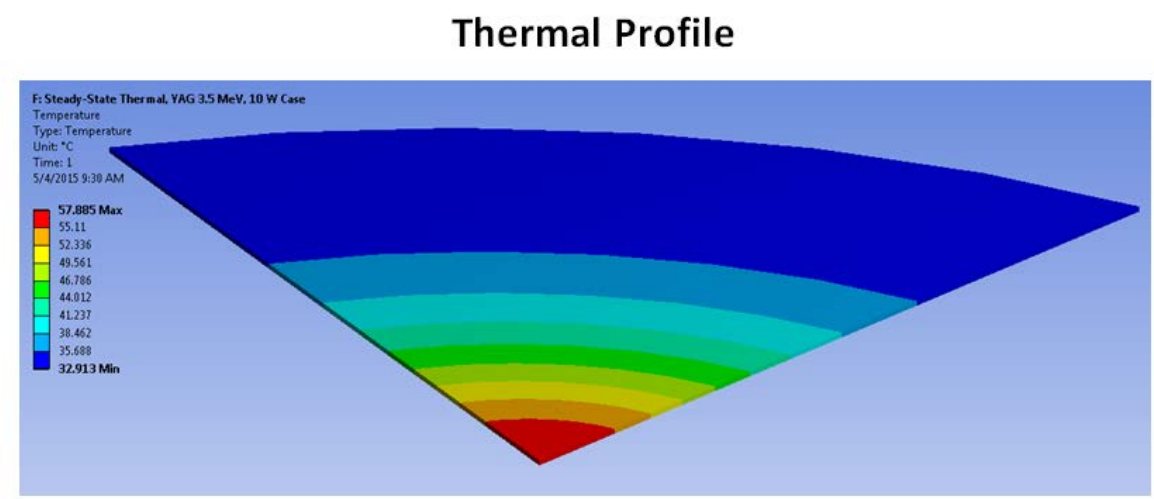

Figure VIII: The steady state temperature profiles for 10 Watts of 3.5 MeV electrons striking the YAG crystal. The beam has a sigma of 3 mm.

The power density for 25 MeV electrons with a 1 mm spot size as a function of radius is displayed in Figure IX for a YAG crystal. The steady state temperature distribution is displayed in Figure X. Ten Watts of beam only cause an 8° C temperature rise in the center of the crystal. Only 0.25% of the initial beam energy is deposited in the YAG, which results in much less energy deposited in the YAG compared to 3.5 MeV.

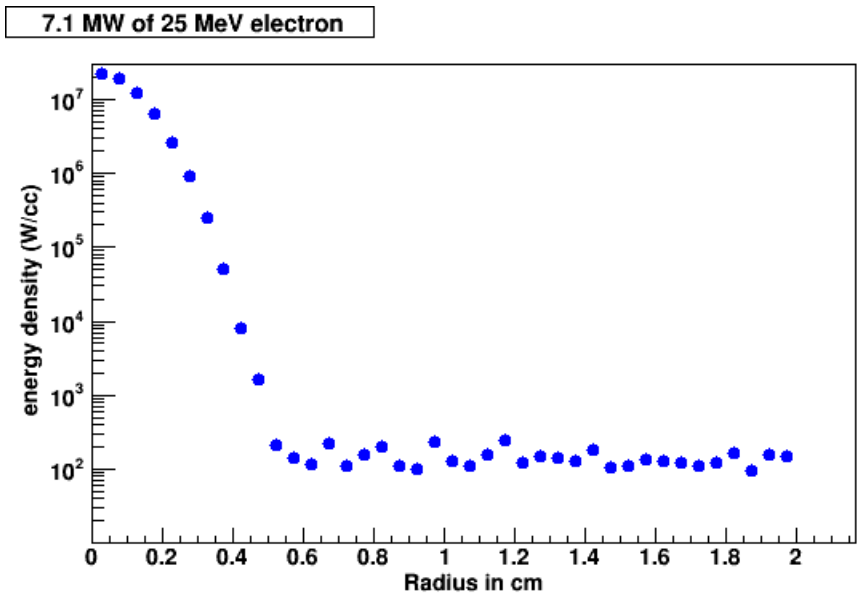

Figure IX: Power density as a function of radius for a 25 MeV electron beam striking a Yag crystal. The beam has a sigma of 0.1cm and a beam power of 7.1 MW. The crystal is 2 cm in diameter and has a thickness of 0.01 cm.

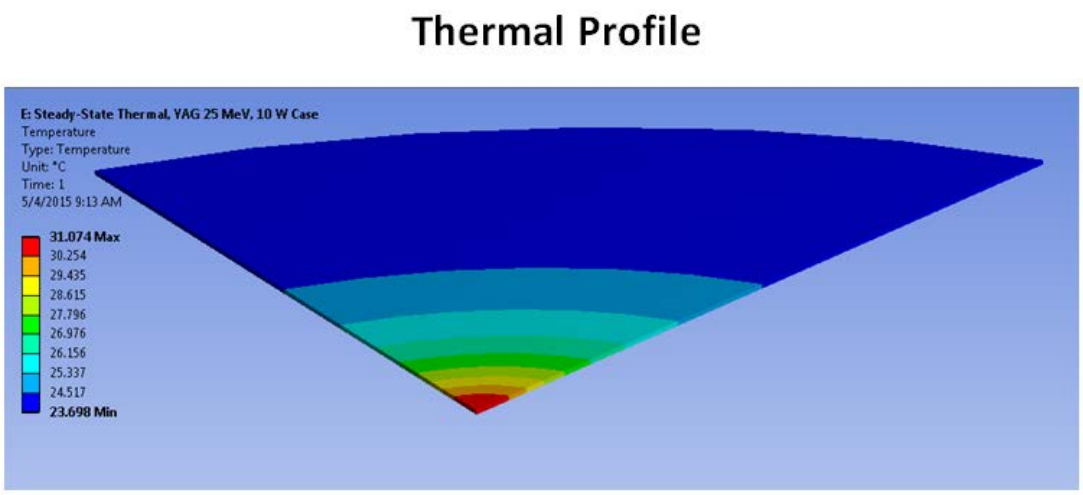

Figure X: Steady state temperature profiles for 10 W of 25 MeV electrons striking a YAG crystal. The beam size is 1mm.

C. Aluminum Vacuum Boxes

The vacuum boxes inside the dipoles are constructed of machined Al boxes welded on the central seam. The first 60° dipole in the loop is a possible location to fault either injected beam[10] or accelerated beam. The energy deposition was approximated assuming that the electron beam struck an Al plate normal to the surface. The thickness of the plate was taken as the side wall of the vacuum box (5.5 mm). For 3.5 MeV 88% of the beam energy was deposited in the walI of

[10] Under normal running conditions injected beam will not be delivered past the extraction dipole for the beam dump.

the Al pipe. In reality the beam will strike the box at an angle and see an effectively thicker wall and have the energy spread over a larger area. For the thermal analysis the flat power density distribution has been mapped onto the curved pipe and the energy increased when the pipe becomes thicker. This should make the calculation conservative. The results for the steady state are shown in Figure IX. The pipe reaches a steady state maximum temperature of 220° C.

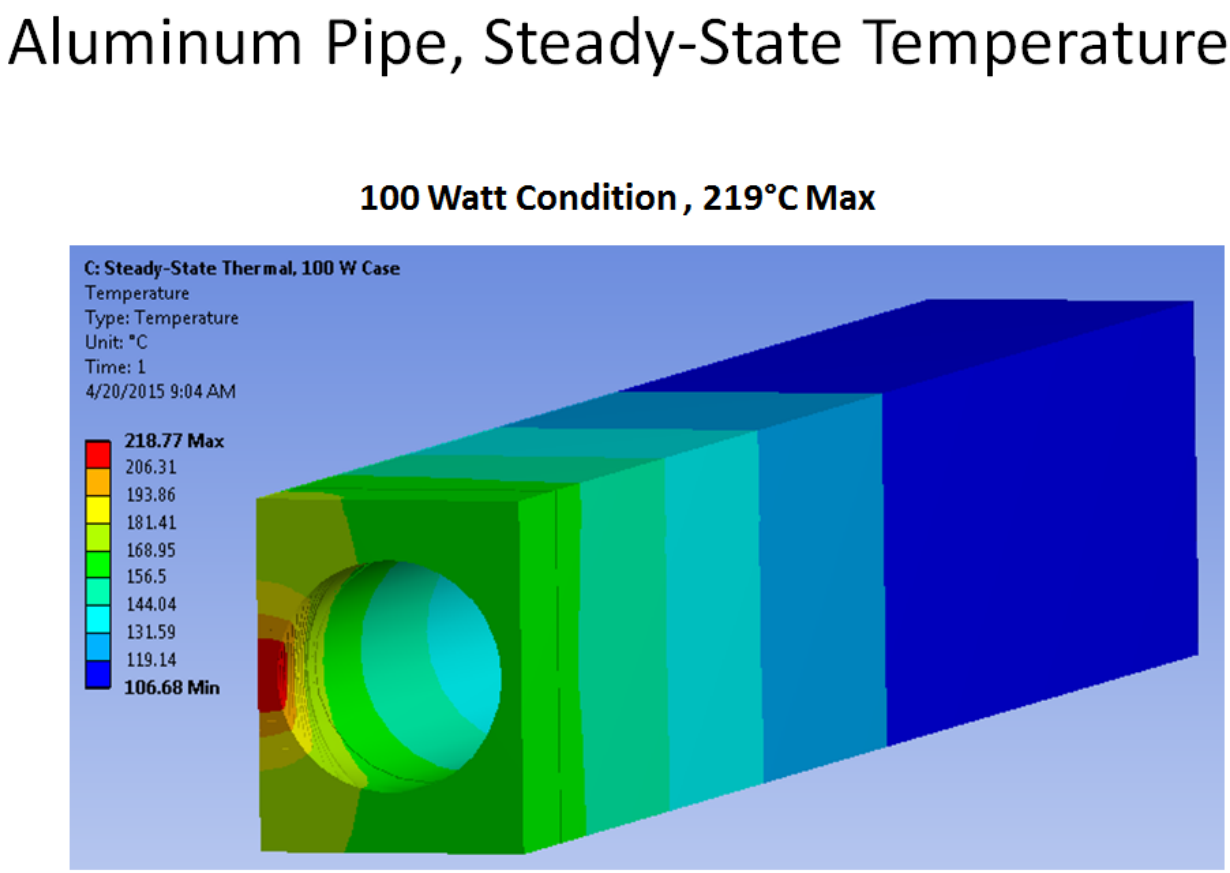

Figure XI: Aluminum pipe struck with 3.5 MeV electrons perpendicular to the wall of the beam pipe.

D. Stainless Steel Pipe

Most of the beam transport is constructed of stainless steel beam pipe[11] with a 0.16 cm wall thickness. Similar to the Al vacuum boxes the 3.5 MeV beam struck the beam pipe at 90° to the surface. The steady state temperature profiles are shown in Figure XII for 10 Watts and a maximum temperature of 165° C is achieved. The 0.16cm wall thickness contains 80% of the electron beam energy. There are probably no locations where the beam tube can be hit at a 90° angle but this is a limiting case. Provided the pipe does not outgas too much it is may be possible

[11] Sections of the loop with quadrupoles have Inconel beam pipes. The thermal properties are similar and the Inconel pipes are not run as a different problem than the stainless steel. The Inconel was chosen for the lower magnetic permeability compared to SS304.

to use close to 20 watts of steady beam on the pipe. Again, it would be the preferred case to operate with the beam striking the beam pipe for short bursts and then have the RCT move to another measuring location.

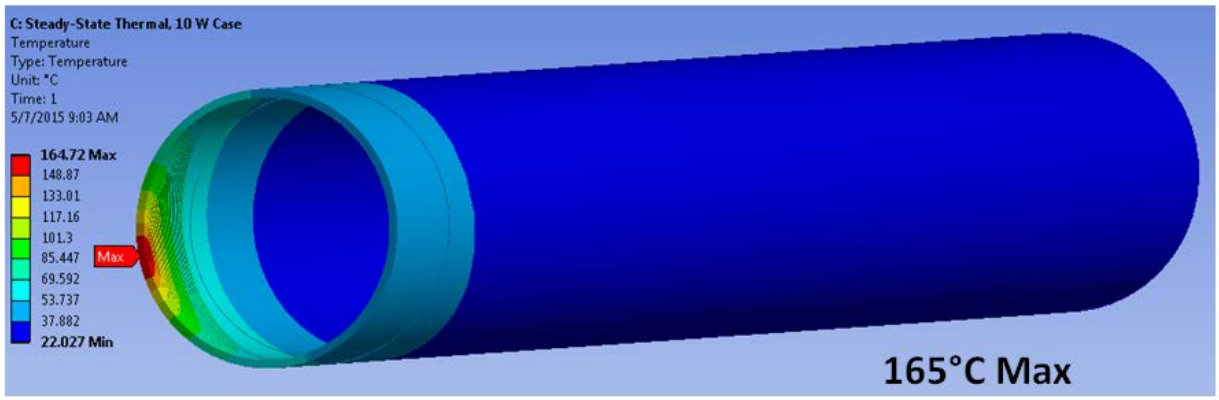

Figure XII: 3.5 MeV striking the wall of the stainless steel beam pipe at 90º. The beam spot is 3 mm in size.

E. Uniform Irradiation of a Stainless Steel Beam pipe

The uniform irradiation of a section of beam pipe can establish upper limits on the amount of beam that can be lost without melting the beam pipe. This can also address the maximum local beam loss that can directly illuminate seams in the shielding. A 10 cm long section of stainless steel pipe had 3.5 electrons strike the interior surface at an angle of 1 milli-radian. The total length of the pipe used in the simulation was 200 cm. The beam has rotational symmetry about the z axis (pipe axis). The power density of for 1 MW of beam is shown in Figure XIII. 94% of the beam power is deposited in the walls the stainless steel beam pipe. The long tail in the forward direction is from scattered electrons and photons. This distribution is then used for input into the thermal analysis.

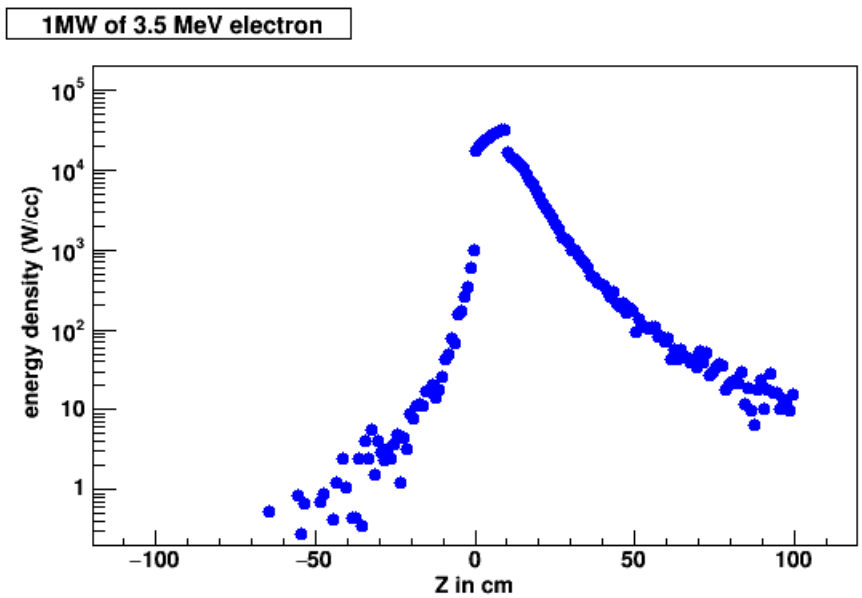

Figure XIII: The power density for 1 MW of 3.5 MeV electrons uniformly striking a 2.54 cm diameter stainless steel beam pipe from z=0 cm to Z = 10 cm.

The distribution in Figure XIII is used in the ANSYS analysis for the beam pipe. The ends of the beam pipe are thermally insulated in the thermal analysis which will add some conservatism especially with lower beam power losses. The distribution can be scaled to estimate the temperatures of the beam pipe that are achieved at beam powers lower than the 1 MW. Figure XIV displays the thermal results for 1 MW of beam. The pipe begins to melt at 0.21 seconds. Structural failure and vacuum pressure issues would likely occur earlier. The same geometry was used for 1kW and 10 kW of beam. The 1 kW achieves a steady state temperature of 660° C. The limiting case for this geometry is 10 kW. The beam pipe reaches a steady state temperature of 1434° C and reaches the melting temperature of 1400° C in 60 seconds. SS304 is considered useable to 815° C which is reached in 13 seconds. The temperature profile and the temperature as a function of time for the 10 kW case is shown in Figure XV.

Figure XIV: The top graph displays the temperature profile of the beam pipe when a 10 cm section is uniformly irradiated with 1MW of 3.5 MeV electrons. The bottom curve displays the maximum temperature as a function of time for the central region.

10 kW, Transient

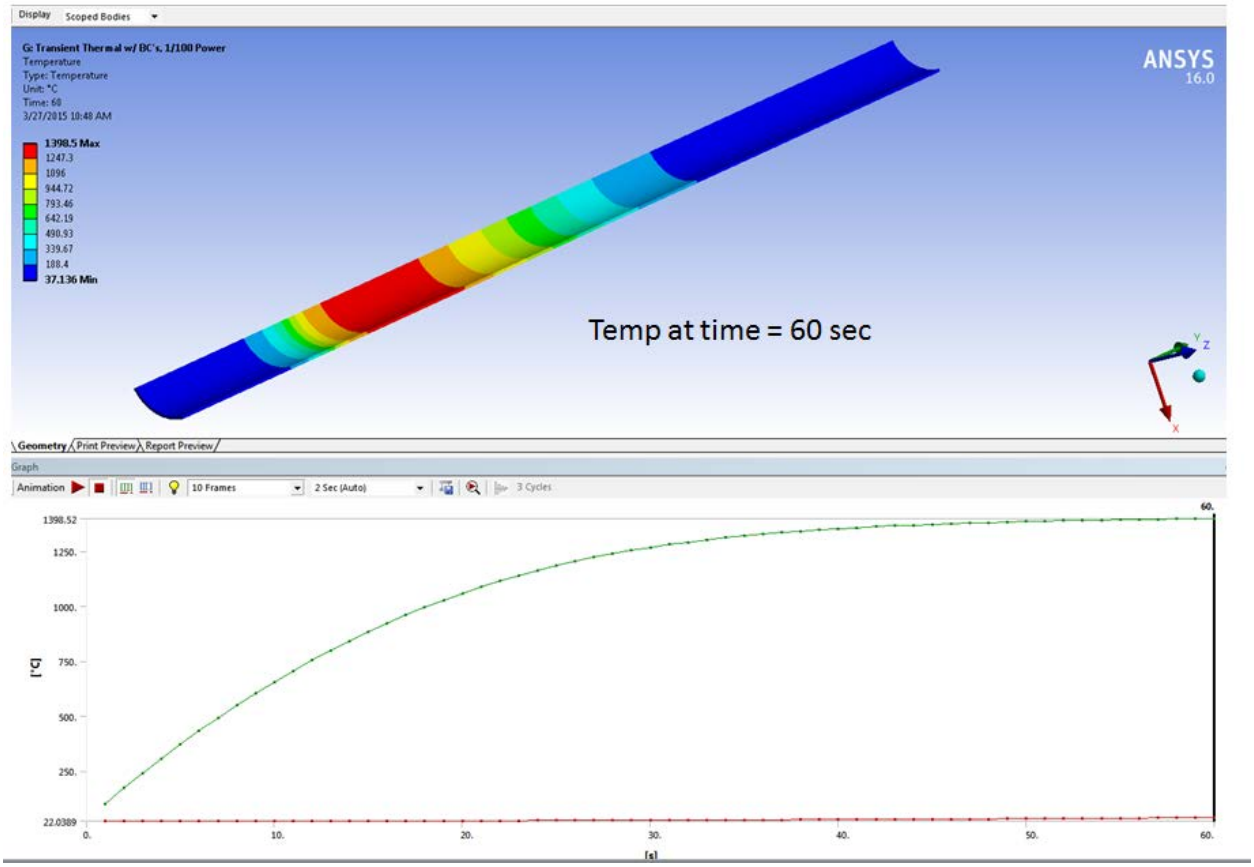

Figure XV: The top graph displays the temperature profile of the beam pipe when a 10 cm section is uniformly irradiated with 10 kW of 3.5 MeV electrons. The bottom curve displays the temperature as a function of time for the central region.

The energy deposition for a stainless steel pipe uniformly irradiated by 25 MeV electrons at an angle of 1 milli-radian is shown in Figure XV. 43% of the beam energy is deposited in the wall of the beam pipe from z=-100 cm to z= 100cm. The 3.5 MeV beam deposited 94%. The longer extent of the energy deposition in the forward direction for 25 MeV beam is evident when comparing Figures XVI and XIII. The peak power density for the 25 MeV beam is 30% that of the 3.5 MeV beam for the same beam power.

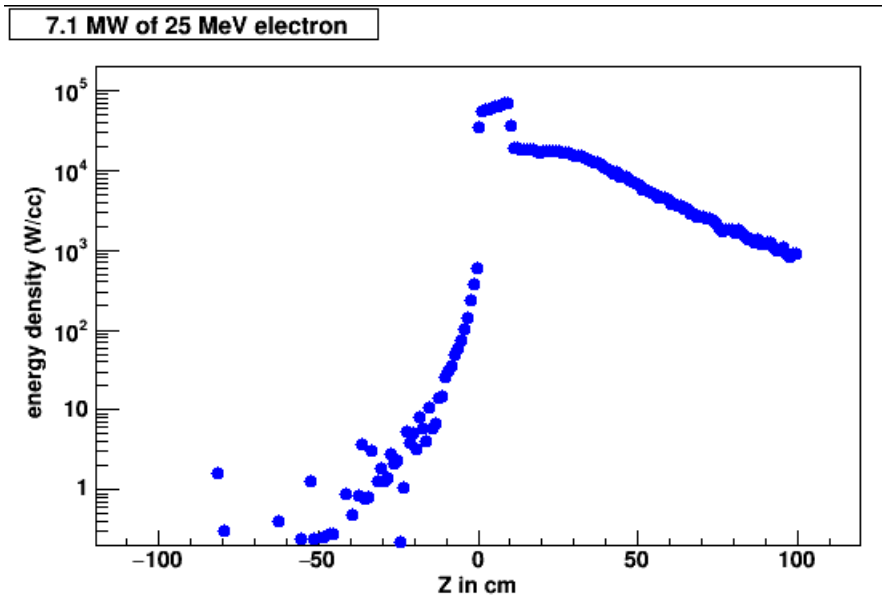

Figure XVI: The power density for 7.1 MW of 25 MeV electrons uniformly striking a 2.54 cm diameter stainless steel beam pipe from z=0 cm to Z = 10 cm.

F. Beam Hitting SS Pipe at 5 degree Angle

In the ERL loop the two methods have been discussed to cause beam scrapping. One is to use the quadrupoles to blow the beam up causing the beam to strike a large area of the beam pipe. The other method is to use the corrector coils in the dipoles to drive the beam into the beam pipe at a relatively shallow angle. With the second method the quadrupoles can be used to provide an enlarged beam size at full energy. The results of several cases are shown in this section.

The power density distribution as a function of distance along the beam pipe is shown in Figure XVII. 93% of the beam energy is deposited in the stainless steel pipe. A steady state temperature of 313° C is achieved for 100 Watts of beam. The temperature profiles are shown in Figure XVIII. Continuous 3.5 MeV beam on the beam pipe should not exceed approximately 50 W.

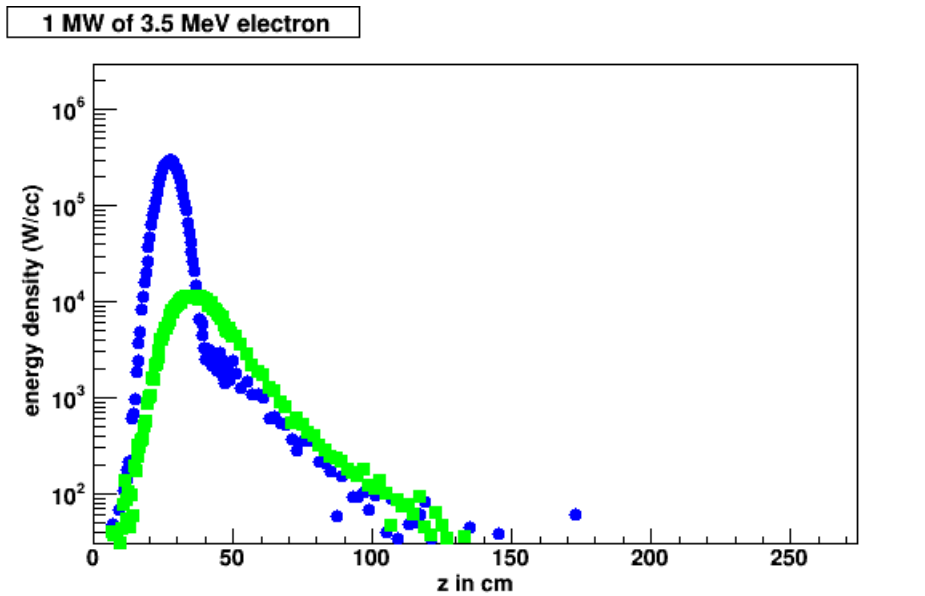

Figure XVII: Power density distribution for 3.5 MeV electrons striking the stainless steel beam pipe at 5 degrees. The beam size is 3mm and starts at the origin. The blue points are in a narrow phi region where the centroid of the beam strikes the beam pipe. The green points are on the opposite side of the beam pipe.

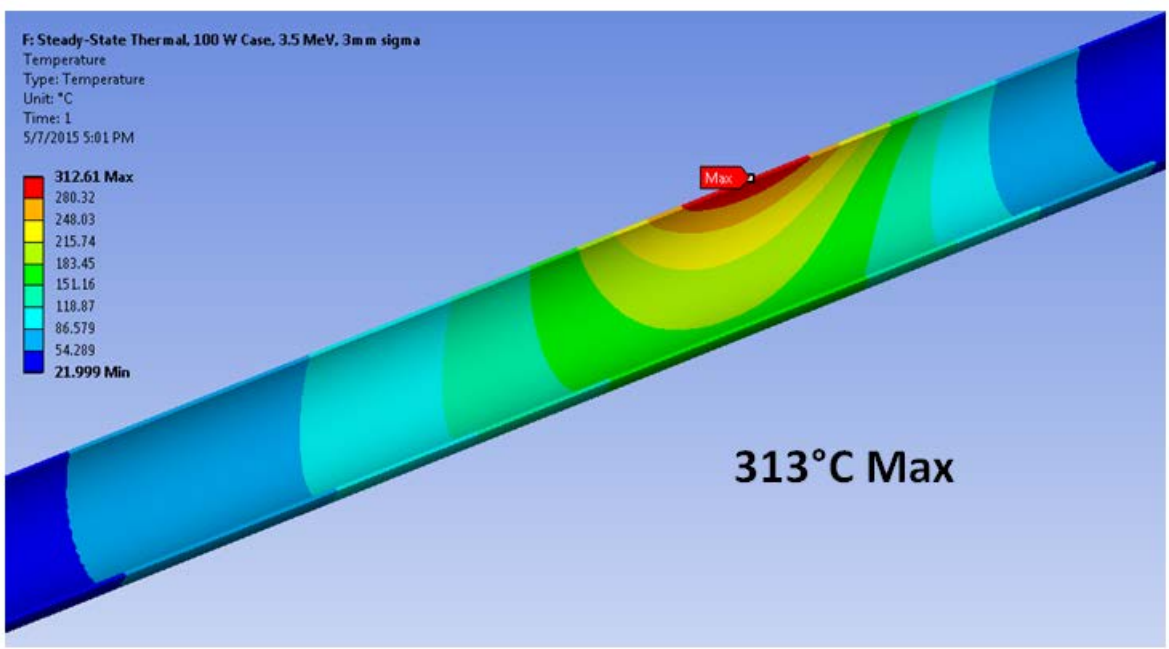

Figure XVIII: Temperature profiles for the stainless steel beam pipe for 3.5 MeV electrons at a 5 degree angle.

The same analysis was conducted for a 25 MeV beam with a 3 mm spot size. Figure XIX displays the power density as a function of distance along the beam pipe. At the higher energy there is less percentage of the total energy deposited in the beam pipe. In this case 42% of the beam energy is deposited. The 3 MeV and 25 MeV distributions are similar with the 25 MeV

having longer tails for energy deposition in the forward direction. For fixed beam power the 3 MeV has a higher power density in the peak than the 25 MeV beam. The steady state temperature profiles are displayed in Figure XX. The peak temperature is 210° C for 100 Watts of beam.

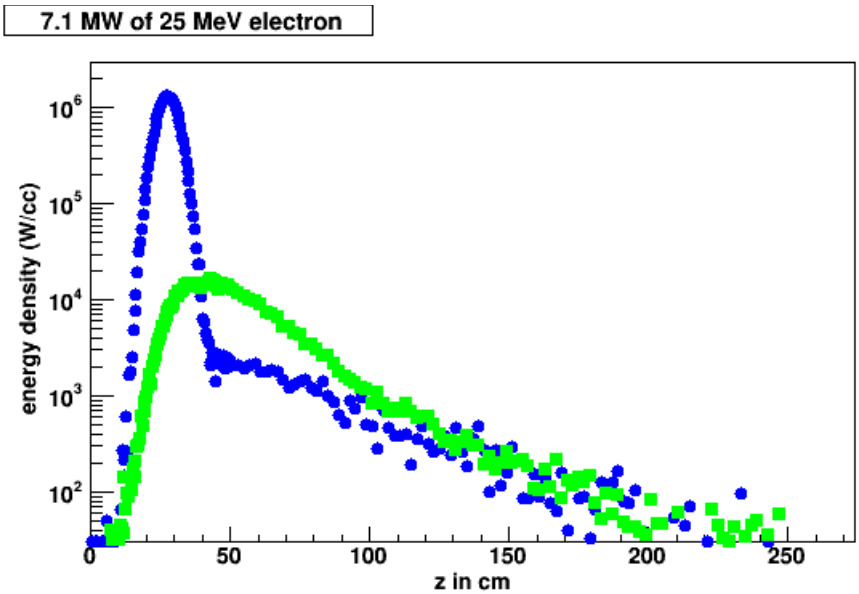

Figure XIX: Power density distribution for 25 MeV electrons striking the stainless steel beam pipe at 5 degrees. The beam size is 3mm and starts at the origin. The blue points are in a narrow phi region where the centroid of the beam strikes the beam pipe. The green points are on the opposite side of the beam pipe.

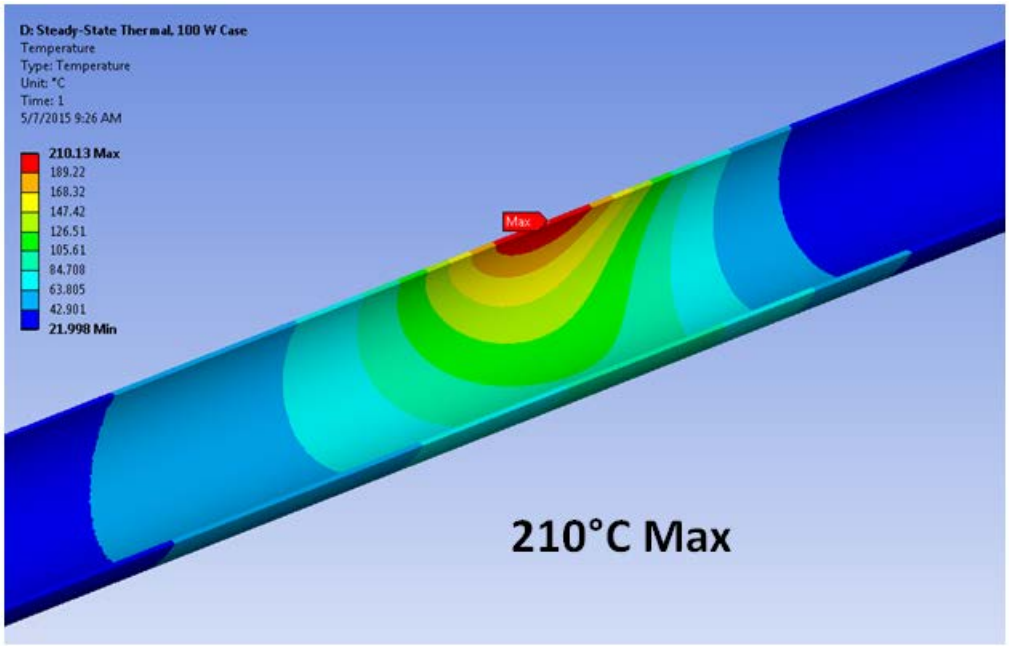

Figure XX: Temperature profiles for the stainless steel beam pipe for 25 MeV electrons at a 5 degree angle with 100 Watts of power. The beam size is 3mm and the maximum temperature is 210º C.

The last case presented is 25 MeV at 5 degrees and a 1mm beam size. The power density distribution is shown in Figure XXI and the steady states temperature profiles in Figure XXII for 10 Watts.

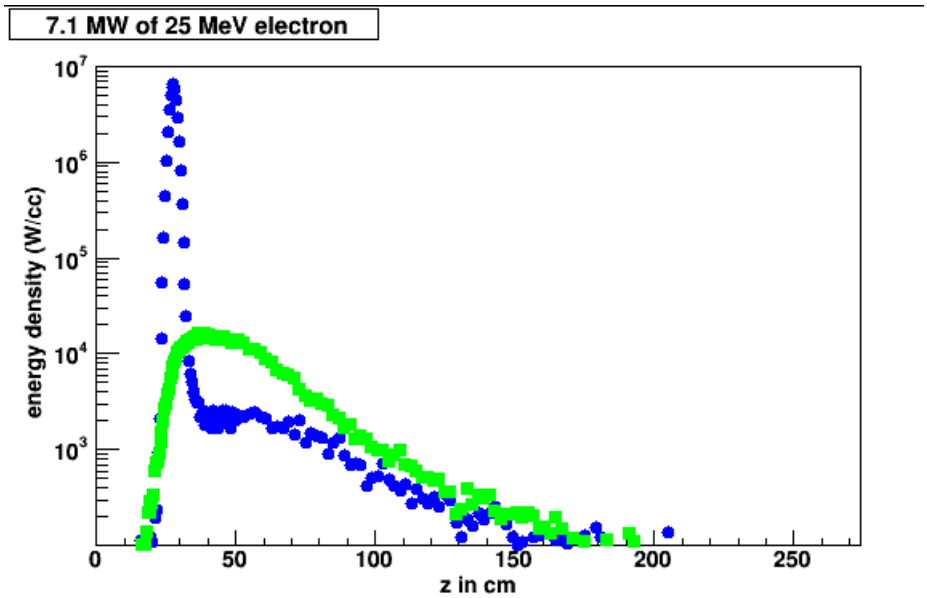

Figure XXI: Same as Figure XIX except a beam size of 1mm.

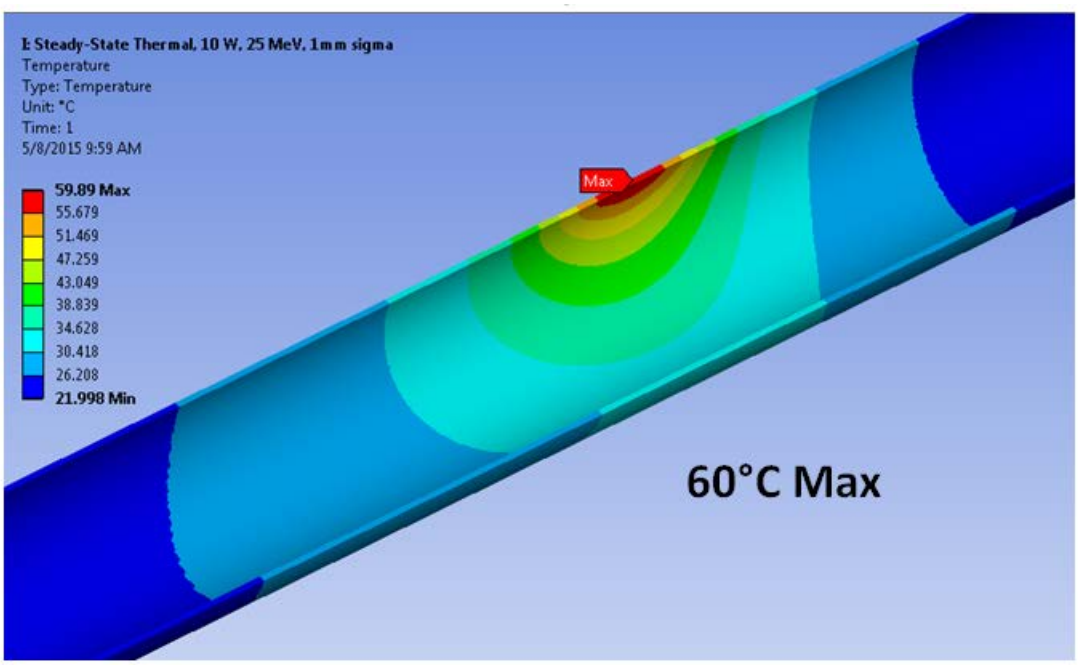

Figure XXII: Same a Figure XX expect 1mm beam spot and 10 Watts of power.

Comments

The size of the electron beam at 25 MeV would typically be 3.5/25 that of the 3.5 MeV beam. For initial 25 MeV beam fault studies the focusing elements can be used to create a beam spot that has a similar area as the 3.5 MeV beam. For the same beam power the higher energy beam will distribute its energy over a larger volume[12] creating a lower power density. For materials that are thin the higher energy beams will deposit a smaller percentage of their energy in the material, which has been demonstrated in the examples shown above. Defocussing the 3.5 MeV beam is also possible if there is a need to escalate to higher beam losses to verify the shielding and there is concern about damage to the components.

The actual beam conditions that will be available for the gun to dump and the loop are not firmly established. Therefore, this analysis was conducted at the ASE limits in energy for the gun beam and the beam accelerated in the five-cell cavity. Either the cases examined here can be interpolate/extrapolated or new cases run to get a more accurate estimate for a specific beam condition.

In most configurations a beam loss of 10 -100 Watt of nearly continuous beam can be used for the shielding and radiation monitor configuration verification. Additionally, the studies can be used to establish MPS trip thresholds to protect the machine.

[12] Primary reason is the greater range of the electrons at increased energy.